Axial current driven by magnetization dynamics in Dirac semimetals

Katsuhisa Taguchi* and Yukio Tanaka
Department of Applied Physics, Nagoya University, Nagoya 464-8603, Japan
and CREST, Japan Science and Technology Corporation (JST), Nagoya 464-8603, Japan
(Received 18 June 2014; revised manuscript received 29 January 2015; published 25 February 2015)

We theoretically study the axial current $\boldsymbol{j}_5$ (defined as the difference between the charge current with opposite helicity) in the magnetic insulator/doped Dirac semimetal using microscopic theory. In the Dirac semimetal, the axial current is induced by the magnetization dynamics, which is produced from the proximity effect of the magnetization of the magnetic insulator. We find that the induced axial current can be detected by using ferromagnetic resonance or the inverse spin Hall effect and can be converted into charge current with no accompanying energy loss. These properties make the Dirac semimetal advantageous for application to low-consumption electronics with new functionality.

DOI: 10.1103/PhysRevB.91.054422 PACS number(s): 85.75.−d, 75.47.−m, 72.25.−b

I. INTRODUCTION

In spintronics, controlling the propagation of the conduction electron spin is a central issue for wide application of low-consumption electronics [1–9]. The flow of the spin, i.e., spin current, is the difference between the charge current of up-spin and that of down-spin and does not accompany any charge current with Joule heating. This spin current is induced by magnetization dynamics at the ferromagnetic metal/normal metal junction [1–3], and it can be converted into the charge current [4–9].

Recently, studies of the axial current, which is defined as the difference between the charge current with right-handed and that with left-handed fermions, have been revived in the field of quantum chromodynamics [10–16]. A stationary axial current $\boldsymbol{j}_5$ exists in the presence of an applied static magnetic field [10–18]. This phenomenon is called the chiral separation effect (CSE) [10–19]. Its origin lies in the difference of helicity between right-handed and left-handed fermions. The helicity $\gamma = \hat{\boldsymbol{\sigma}} \cdot \hat{\boldsymbol{p}}$ indicates the relative angle between the direction of the spin $\hat{\boldsymbol{\sigma}}$ and that of the momentum $\hat{\boldsymbol{p}}$ of chiral fermions. The helicity of right-handed fermions is $\gamma = +1$, whereas that of left-handed ones is $\gamma = -1$, but both spins are parallel to each other along the applied magnetic field $\boldsymbol{H}$ [Fig. 1(a)]. Thus, it is remarkable that charge current vanishes in the presence of $\boldsymbol{j}_5$ only when the difference between the numbers of fermions with each helicity are zero [10–16], and $\boldsymbol{j}_5$ satisfies the conservation law $\partial_t \rho_5 + \nabla \cdot \boldsymbol{j}_5 = 0$, where ρ_5 is the axial charge density. Recently, focus has been on the detection of the axial current and has relied on heavy-ion collision experiments [20].

It is noted that there is a similarity between the axial current and the spin current. Here the axial current transports without accompanying charge current. In fact, the axial current can be decomposed into counterpropagating charge flow with opposite helicity, whose spins are polarized along the applied magnetic field direction. Therefore, the axial current is controlled not only by the static magnetic field but also by the magnetization dynamics, which is used to generate spin current in spintronics. Moreover, an advantage of using the axial current is its conservative value in contrast to spin current. One can thus expect new spin transport via the axial current in condensed matter physics. Recently, a candidate material hosting massless Dirac fermions, e.g., the Dirac semimetal (DS), has been suggested in condensed matter physics [21–23]. Therefore, studying the transport properties of DS in the context of axial current is of interest.

In this paper, we study the axial current, which is driven by CSE due to the magnetization dynamics (DCSE) in the junction of three-dimensional bulk doped DS/magnetic insulator (MI) [Fig. 1(b)]. Here the axial current is calculated by using the Green's functions. The present DCSE offers the advantage of our being able to control the magnitude of the axial current by means of ferromagnetic resonance in the MI and is useful for detecting the axial current in condensed matter physics. Since the present axial current can be transformed into a charge current, this axial-current-based electronics, *axitronics*, enables applications for low-consumption electricity transmission.

II. MODEL

We consider a doped DS/MI junction, as shown in Fig. 1(b), where the the magnetization in the MI penetrates from the MI into the doped DS. Then, an effective localized spin is generated in the doped DS in the length scale $\lambda \gg \ell$ as shown in the gray area of Fig. 1(b), where ℓ is the electron mean-free path in the doped DS. We assume that the electronic properties of doped DS do not change significantly by this proximity effect. The setup and assumptions are similar to those of spin-pumping generation in metallic spintronics [3,8]. The total Hamiltonian in the gray area of Fig. 1(b) is given by

$$\mathcal{H} = \mathcal{H}_{\mathrm{D}} + \mathcal{H}_{\mathrm{ex}} + V_{\mathrm{i}}. \tag{1}$$

Here, $\mathcal{H}_{\mathrm{D}}$ is a Hamiltonian of the three-dimensional bulk doped DS, where the inversion and time-reversal symmetries are satisfied. The massless four-component Dirac Hamiltonian $\mathcal{H}_{\mathrm{D}}$ can be divided into a 2×2 matrix corresponding to each helicity sector γ as $\mathcal{H}_{\mathrm{D}} = \sum_{\gamma=\pm} \mathcal{H}_{\mathrm{D},\gamma}$:

$$\mathcal{H}_{\mathrm{D},\gamma} = \int d\boldsymbol{x}\, \psi_\gamma^\dagger [-i\hbar v_{\mathrm{F},\gamma} \boldsymbol{\nabla} \cdot \hat{\boldsymbol{\sigma}} - \epsilon_{\mathrm{F}}] \psi_\gamma, \tag{2}$$

where $\psi_\gamma \equiv \psi_\gamma(\boldsymbol{x},t) = {}^t(\psi_{\gamma,\uparrow} \psi_{\gamma,\downarrow})$, and $\psi_\gamma^\dagger$ are the annihilation and creation operators of electrons of each γ, respectively

*taguchi@rover.nuap.nagoya-u.ac.jp

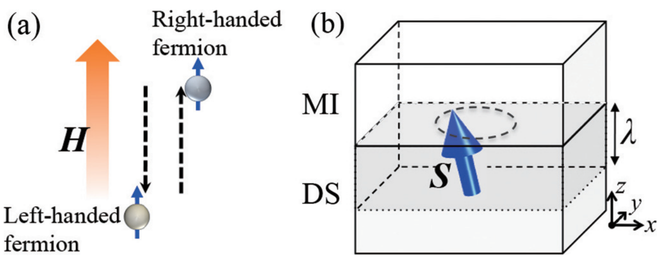

FIG. 1. (Color online) (a) Schematic illustration of the CSE. (b) A setup of the doped DS/MI junction for the axial current generation. Since the magnetization in the MI can penetrate into the doped DS in the length scale λ, the effective localized spin $\boldsymbol{S}$ can be generated in the doped DS, as shown in the gray area.

(where indices $\uparrow$ and $\downarrow$ represent spin), $\epsilon_{\rm F}$ is the Fermi energy, and $v_{{\rm F},\gamma} = \gamma v_{\rm F}$ is the Fermi velocity. $\hat{\boldsymbol{\sigma}}$ represents the Pauli matrices in spin space. The second term of Eq. (1), $\mathcal{H}_{\rm ex} = \sum_{\gamma=\pm} \mathcal{H}_{{\rm ex},\gamma}$, shows the exchange coupling. Here $\mathcal{H}_{{\rm ex},\gamma}$ can be given by

$$\mathcal{H}_{{\rm ex},\gamma} = -\int d\boldsymbol{x}\, J_{\rm ex} \psi_\gamma^\dagger \boldsymbol{S}\cdot\hat{\boldsymbol{\sigma}}\psi_\gamma, \tag{3}$$

where $J_{\rm ex} > 0$ is the exchange coupling constant, and $\boldsymbol{S} \equiv \boldsymbol{S}(\boldsymbol{x},t)$ is the effective localized spin in the doped DS. The third term of Eq. (1), $V_{\rm i} = u_{\rm i}\sum_\gamma \sum_{j=1}^{N_i} \int d\boldsymbol{x}\,\delta(\boldsymbol{x}-\boldsymbol{r}_j)\psi_\gamma^\dagger\psi_\gamma$, represents nonmagnetic impurity scattering, which causes a relaxation time τ of the transport of conduction electrons in the DS. Here $u_{\rm i}$, $\boldsymbol{r}_j$, and $N_{\rm i}$ are the potential energy, the position, and the number of impurities, respectively.

We calculate $\boldsymbol{j}_5$ in the linear response to $\boldsymbol{S}$ by treating $\mathcal{H}_{{\rm ex},\gamma}$ as a perturbation within the diffusive transport regime, $J_{\rm ex} \ll \hbar/\tau$ [3], which can be allowed in a disordered doped DS. To consider $\boldsymbol{j}_5$, we will calculate the charge current density of each helicity sector $\boldsymbol{j}_\gamma$. Here $\boldsymbol{j}_\gamma = -ev_{{\rm F},\gamma}\langle\psi_\gamma^\dagger\boldsymbol{\sigma}\psi_\gamma\rangle$ is defined from the conservation law $\dot{\rho}_\gamma = -\nabla\cdot\boldsymbol{j}_\gamma$, where $\rho_\gamma \equiv -e\langle\psi_\gamma^\dagger\psi_\gamma\rangle$ is the charge density of γ. The current is represented by using the same space and time of lesser Green's functions $G_\gamma^< = \langle\psi_\gamma^\dagger\psi_\gamma\rangle/(-i\hbar)$ as $j_{i,\gamma}(\boldsymbol{x},t) = i\hbar e v_{{\rm F},\gamma}{\rm tr}[\hat{\sigma}_i G_\gamma^<(\boldsymbol{x},t:\boldsymbol{0},0)]$. $j_{\mu,\gamma}$ in the linear response to $\boldsymbol{S}$ is given by

$$j_{i,\gamma} = \frac{-i\hbar J_{\rm ex} e v_{{\rm F},\gamma}}{V}\sum_{\boldsymbol{q},\Omega} e^{-i(\boldsymbol{q}\cdot\boldsymbol{x}-\Omega t)}\Pi_{ij,\gamma}(\boldsymbol{q},\Omega)S^j_{\boldsymbol{q},\Omega}, \tag{4}$$

$$\Pi_{ij,\gamma} = \frac{1}{V}\sum_{\boldsymbol{k},\omega}{\rm tr}\big[\hat{\sigma}_i g_{\boldsymbol{k}-\frac{\boldsymbol{q}}{2},\omega-\frac{\Omega}{2},\gamma}\hat{\Lambda}_{j,\gamma} g_{\boldsymbol{k}+\frac{\boldsymbol{q}}{2},\omega+\frac{\Omega}{2},\gamma}\big]^<, \tag{5}$$

where $\Pi_{ij,\gamma}$ is the spin-spin correlation function and $\hat{\Lambda}_{j,\gamma}$ is the vertex function of $V_{\rm i}$. Here $\boldsymbol{q}$ and Ω are the momentum and the frequency of $\boldsymbol{S}$, respectively. $g^<_{\boldsymbol{k},\omega,\gamma}$ is the nonperturbative Green's function of $\mathcal{H}_{{\rm D},\gamma}$ including $V_{\rm i}$ with $g^r_{\boldsymbol{k},\omega,\gamma} = [\hbar\omega + \epsilon_{\rm F} - \hbar v_{{\rm F},\gamma}\boldsymbol{k}\cdot\hat{\boldsymbol{\sigma}} + i\hbar/(2\tau)]^{-1}$. Here g^r (g^a) is the retarded (advanced) Green's function. $\hbar/(2\tau) = n_i u_i^2 \nu_e/4$ is the self-energy of $V_{\rm i}$, where $n_{\rm i} = N_{\rm i}/V$ is the concentration of impurities, ν_e is the density of states at $\epsilon_{\rm F}$, and V is the system volume. We calculate $\Pi_{ij,\gamma}$ by using $g^<_{\boldsymbol{k},\omega,\gamma} = f_\omega(g^a_{\boldsymbol{k},\omega,\gamma} - g^r_{\boldsymbol{k},\omega,\gamma})$ [24], where f_ω is the Fermi distribution function. Now, we only consider the nonequilibrium component of $j_{i,\gamma}$. Besides, we assume that $\boldsymbol{S}$ slowly varies in space (i.e., $q\ell \ll 1$) and time (i.e., $\Omega\tau \ll 1$) in the doped DS. Then, the dominant contribution is obtained by using $\hbar/(\epsilon_{\rm F}\tau) \ll 1$, expanding with $q\ell \ll 1$ and $\Omega\tau \ll 1$, and assuming isotropic $\boldsymbol{q}$ as

$$\Pi_{ij,\gamma}(\boldsymbol{q},\Omega) = -\frac{\nu_e\Omega\tau}{2\hbar}\left[\delta_{ij} - \frac{\frac{3}{2}Dq_iq_j}{\frac{3}{2}Dq^2 + i\Omega}\right], \tag{6}$$

where $D = v_{\rm F}^2\tau/3$ is the diffusion constant. Here the response function $\Pi_{ij,\gamma}$ gives

$$j_{i,\gamma} = \frac{ev_{{\rm F},\gamma}J_{\rm ex}\nu_e}{2V}\sum_{\boldsymbol{q},\Omega} e^{i(\Omega t-\boldsymbol{q}\cdot\boldsymbol{x})}i\Omega\tau\left[\delta_{ij} - \frac{\frac{3}{2}Dq_iq_j}{\frac{3}{2}Dq^2+i\Omega}\right]S^j_{\boldsymbol{q},\Omega}. \tag{7}$$

The second term in Eq. (7) is given by ρ_γ, which is calculated by using $\Pi_{0j,\gamma}$ as

$$\rho_\gamma = -\tfrac{1}{2}ev_{{\rm F},\gamma}J_{\rm ex}\nu_e\tau\nabla\cdot\partial_t\langle\boldsymbol{S}\rangle_{\rm D}, \tag{8}$$

where $\langle\boldsymbol{S}\rangle_{\rm D}$ is defined by the convolution of $\boldsymbol{S}$ and a diffusive propagation function $\mathcal{D}$ [25] given by $\langle\boldsymbol{S}\rangle_{\rm D} \equiv \int_{-\infty}^{\infty}dt'\int d\boldsymbol{x}'\mathcal{D}(\boldsymbol{x}-\boldsymbol{x}',t-t')\boldsymbol{S}(\boldsymbol{x}',t')$ and $\mathcal{D}(\boldsymbol{x},t) \equiv \frac{1}{V}\sum_{\boldsymbol{q},\Omega}e^{-i(\boldsymbol{q}\cdot\boldsymbol{x}-\Omega t)}[\frac{3}{2}Dq^2+i\Omega]^{-1}$. Therefore, we obtain

$$\boldsymbol{j}_\gamma = \frac{ev_{{\rm F},\gamma}J_{\rm ex}\nu_e\tau}{2}\partial_t\boldsymbol{S} - \frac{3}{2}D\nabla\rho_\gamma. \tag{9}$$

It is noted that, from Eqs. (7) and (8), ρ_γ and $\boldsymbol{j}_\gamma$ satisfy the conservation law $\dot{\rho}_\gamma + \nabla\cdot\boldsymbol{j}_\gamma = 0$ [26].

III. AXIAL CURRENT DUE TO MAGNETIZATION DYNAMICS

Now, we turn to a discussion of the charge current density and the charge density induced by magnetization dynamics after the summation over the index of the helicity γ. Since $\boldsymbol{j}_\gamma$ is proportional to γ from Eq. (7), the directions of $\boldsymbol{j}_+$ and $\boldsymbol{j}_-$ are opposite to each other. In the same way, Eq. (8) shows $\rho_+ = -\rho_-$. Thus, the induced total charge current density and charge density vanish:

$$\boldsymbol{j}_+ + \boldsymbol{j}_- = 0, \quad \rho_+ + \rho_- = 0. \tag{10}$$

However, from Eqs. (8) and (9), the axial current density $\boldsymbol{j}_5 \equiv \boldsymbol{j}_+ - \boldsymbol{j}_-$ and the axial charge density $\rho_5 \equiv \rho_+ - \rho_-$ are given by

$$\boldsymbol{j}_5 = ev_{\rm F}J_{\rm ex}\nu_e\tau\partial_t\boldsymbol{S} - \tfrac{3}{2}D\nabla\rho_5, \tag{11}$$

$$\rho_5 = -ev_{\rm F}J_{\rm ex}\nu_e\tau\nabla\cdot\partial_t\langle\boldsymbol{S}\rangle_{\rm D}. \tag{12}$$

From Eqs. (10) and (11), $\boldsymbol{j}_5$ can be driven by the DCSE. Here $\boldsymbol{j}_5$ can be decomposed into a local component $\boldsymbol{j}_5^{\rm L}$ and a diffusive one $\boldsymbol{j}_5^{\rm D}$ with $\boldsymbol{j}_5 \equiv \boldsymbol{j}_5^{\rm L} + \boldsymbol{j}_5^{\rm D}$. The first term of Eq. (11), $\boldsymbol{j}_5^{\rm L}$, is proportional and parallel to $\partial_t\boldsymbol{S}$. $\boldsymbol{j}_5^{\rm L}$ corresponds to a local axial current. The second term of Eq. (11), $\boldsymbol{j}_5^{\rm D}$, is driven by the spatial gradient of ρ_5 and is parallel to its gradient. The axial charge density ρ_5 is triggered by the time and spatial dependence of the localized spin, $\nabla\cdot\partial_t\langle\boldsymbol{S}\rangle_{\rm D}$ [27]. Here $\langle\boldsymbol{S}(\boldsymbol{x},t)\rangle_{\rm D}$ expresses the diffusion propagation by random impurity scattering in the doped DS. Thus, $\boldsymbol{j}_5^{\rm D}$ corresponds to a diffusive axial current. $\boldsymbol{j}_5^{\rm L}$ and $\boldsymbol{j}_5^{\rm D}$ coexist in the case with

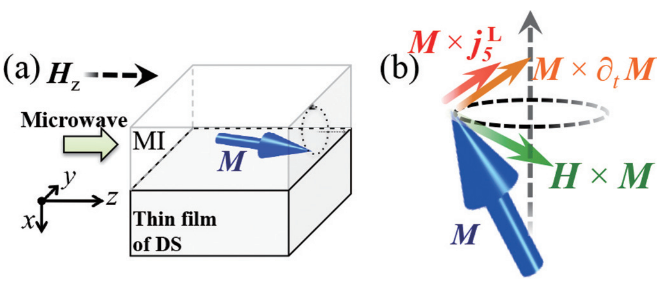

FIG. 2. (Color online) (a) Schematic diagram of the axial current generation and ferromagnetic resonance. (b) Schematic illustration of the torque acting the magnetization at the interface between the MI and the thin film of the doped DS in Fig. 2(a). The green arrow denotes field-driven torque and the orange and red arrow represent the damping torque.

$\lambda \gg \ell$. On the other hand, if $\lambda \ll \ell$ is satisfied, the magnitude of $\boldsymbol{j}_5^{\rm L}$ could be dominant compared to $\boldsymbol{j}_5^{\rm D}$.

IV. DETECTION OF LOCAL AXIAL CURRENT

We phenomenologically consider the magnetization dynamics after the axial current generation in the MI/doped DS junction, where a static magnetic field parallel to the z axis and ac magnetic field along the z axis due to microwave irradiation are applied in the MI as shown in Fig. 2(a). The magnetization dynamics at the interface between the MI and the DS are given from the Landau-Lifshitz-Gilbert equation as

$$\partial_t \boldsymbol{M} = \gamma\mu \boldsymbol{H}\times\boldsymbol{M} + \frac{\alpha_{\rm G}}{M}\boldsymbol{M}\times\partial_t\boldsymbol{M} + \boldsymbol{\mathcal{T}}_{\rm e}, \quad (13)$$

where $\boldsymbol{M}(\boldsymbol{x},t) = -(M/S)\boldsymbol{S}$ is the magnetization in the MI at the interface, M is its magnitude, S is the magnitude of the localized spin, μ is permeability, γ is the gyromagnetic ratio, $\boldsymbol{H}$ is the applied magnetic fields, $\alpha_{\rm G}$ is the Gilbert damping constant, and $\boldsymbol{\mathcal{T}}_{\rm e} = \frac{2J_{\rm ex}}{\hbar}\boldsymbol{M}\times\boldsymbol{s}$ is the spin-transfer torque. Because of spin-momentum locking, spin density in the doped DS, $\boldsymbol{s}$, satisfies $\boldsymbol{s} = -\frac{1}{2ev_{\rm F}}\boldsymbol{j}_5$. Therefore, the spin-transfer torque, $\boldsymbol{\mathcal{T}}_{\rm e} = \frac{-J_{\rm ex}}{\hbar e v_{\rm F}}(\boldsymbol{M}\times\boldsymbol{j}_5^{\rm L} + \boldsymbol{M}\times\boldsymbol{j}_5^{\rm D})$, is described by the axial current represented from Eq. (11) as

$$\boldsymbol{\mathcal{T}}_{\rm e} = \frac{J_{\rm ex}^2\nu_e\tau S}{\hbar M}\left[\boldsymbol{M}\times\partial_t\boldsymbol{M} + \frac{3}{2}D\boldsymbol{M}\times\nabla\left(\nabla\cdot\partial_t\langle\boldsymbol{M}\rangle_{\rm D}\right)\right]. \quad (14)$$

The first term of Eq. (14) corresponds to $\boldsymbol{M}\times\boldsymbol{j}_5^{\rm L}$. This torque enhances the relaxation of the magnetization dynamics [Fig. 2(b)] and modifies the damping coefficient from $\alpha_{\rm G}$ into $\alpha_{\rm G} + J_{\rm ex}^2\nu_e\tau S/\hbar$ in Eq. (13). The second term of Eq. (14) is caused by $\boldsymbol{M}\times\boldsymbol{j}_5^{\rm D}$; its direction is perpendicular to $\boldsymbol{M}$ and $\nabla[\nabla\cdot\partial_t\langle\boldsymbol{M}\rangle_{\rm D}]$, where $\langle\boldsymbol{M}\rangle_{\rm D} \equiv \int d\boldsymbol{x}'\mathcal{D}(\boldsymbol{x}-\boldsymbol{x}')\boldsymbol{M}(\boldsymbol{x}')$ includes the contribution from the magnetization $\boldsymbol{M}(\boldsymbol{x}')$, which penetrates into the doped DS. From Eqs. (13) and (14), the torque $\boldsymbol{M}\times\boldsymbol{j}_5^{\rm L}$ can be detected by using magnetic resonance in the setup shown in Fig. 2(a), since the damping constant is experimentally estimated from the half-width value of the permeability at magnetic resonance [28,29]. For example, we consider the setup of the MI / doped DS, where the thickness of the thin film of the doped DS is smaller than the length scale λ as shown in Fig. 2(a). Besides, the magnetization at the interface is spatially uniform [30]. Then, the diffusive axial current $\boldsymbol{j}_5^{\rm D}$ could be negligibly smaller than one due to the local axial current $\boldsymbol{j}_5^{\rm L}$ at the interface between the MI and the doped DS. Therefore, we expect that the spin-transfer torque by $\boldsymbol{j}_5^{\rm L}$ could be dominant compared with one due to $\boldsymbol{j}_5^{\rm D}$ at the interface. As a result, the half-width value ΔH of the ferromagnetic resonance is changed by the torque $\boldsymbol{M}\times\boldsymbol{j}_5^{\rm L}$ as

$$\Delta H = 2\omega_0\left(\alpha_{\rm G} + J_{\rm ex}^2\nu_e\tau S/\hbar\right). \quad (15)$$

This equation means that before and after the generation of $\boldsymbol{j}_5^{\rm L}$, the half-width value changes from $2\omega_0\alpha_{\rm G}$ by $2\omega_0 J_{\rm ex}^2\nu_e\tau S/\hbar$, where ω_0 is the resonance frequency. When we choose the parameters $J_{\rm ex}/\epsilon_{\rm F} = 0.01$, $\tau = 6\times10^{-14}$ s, $\epsilon_{\rm F}\nu_e = 1$, and $S = 5/2$, the change in damping is estimated as $J_{\rm ex}^2\nu_e\tau S/\hbar \sim 2\times10^{-3}$. The order of $\alpha_{\rm G}$ is reported as 10^{-3} in ferromagnets [29] and 10^{-5} in MIs [6]. Therefore, the change of the half-width value should be measurable.

V. DETECTION OF DIFFUSIVE AXIAL CURRENT

To discuss an experimental setup for the detection of the diffusive axial current $\boldsymbol{j}_5^{\rm D}$, we consider the property of $\boldsymbol{j}_5^{\rm D}$ in the junction [Fig. 1(b)] for $\lambda \gg \ell$. From Eq. (11), $\boldsymbol{j}_5^{\rm D}$ obeys the diffusive equation [31],

$$\left(\partial_t - \frac{3}{2}D\nabla^2\right)\boldsymbol{j}_5^{\rm D} = \frac{3ev_{\rm F}J_{\rm ex}\nu_e}{2}D\partial_t\nabla(\nabla\cdot\boldsymbol{S}). \quad (16)$$

From Eq. (16), $\boldsymbol{j}_5^{\rm D}$ is produced by $\partial_t\nabla(\nabla\cdot\boldsymbol{S})$ in the doped DS and $\boldsymbol{j}_5^{\rm D}$ propagates diffusively and isotropically in the doped DS. Here $\boldsymbol{j}_5^{\rm D}$ can be interpreted as the diffusive conduction electron spin $\boldsymbol{s}^{\rm D}$ with $\boldsymbol{s}^{\rm D} = \boldsymbol{j}_5^{\rm D}/(-2ev_{\rm F})$, because of the spin-momentum locking in the doped DS. Then, Eq. (16) can be regarded as a spin-diffusive equation in the doped DS. Therefore, from Eq. (16), we expect that the diffusive propagation of $\boldsymbol{s}^{\rm D} \propto \boldsymbol{j}_5^{\rm D}$ can be accumulated at the edge in the doped DS. The accumulation could be electrically detected in the MI/doped DS/normal metal (NM) junction (Fig. 3) by using the method established in spintronics [5–9]. For example, we assume that in the junction, NM has a spin-orbit interaction and the localized spin $\boldsymbol{S}$ in the doped DS varies in time and space along x axis. We expect that $\boldsymbol{S}$ could be produced when the spatial dependence of the magnetization of the MI behaves like the spin wave. Besides, the spin wave propagates along the x axis (e.g., $\boldsymbol{S} - S_z\boldsymbol{z} \propto {\rm Re}[e^{iq_x x}(1,i,0)]$). Then, $\partial_t\nabla(\nabla\cdot\boldsymbol{S})$ is parallel to the x axis and induces $\boldsymbol{s}^{\rm D}\|\boldsymbol{x}$ in the doped DS. The

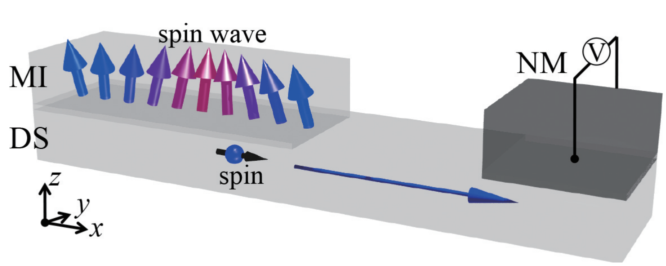

FIG. 3. (Color online) Geometry for $\boldsymbol{j}_5^{\rm D}$ in the MI/doped DS/NM junction.

induced spin $\boldsymbol{s}^{\mathrm{D}} \| \boldsymbol{x}$ is isotropically propagating in the doped DS and accumulating at the edge of the doped DS. One of the accumulated spins could be sinked from the doped DS into the NM along the z direction [5–9] (flow of spin $\boldsymbol{I}_s \| \boldsymbol{z}$ and its spin $\boldsymbol{s}^{\mathrm{D}} \| \boldsymbol{x}$ in the NM). Then, $\boldsymbol{I}_s$ in the NM can be converted into charge current $\boldsymbol{j} \propto \boldsymbol{s}^{\mathrm{D}} \times \boldsymbol{I}_s$ parallel to the $-y$ axis through the inverse spin Hall effect [5–9]. We notice that $\boldsymbol{j}_5^{\mathrm{D}}$ propagates without any accompanying charge current [see Eq. (10)] [32] and can be converted into the charge current. Therefore, the diffusive axial current could be detected electrically and could be useful for an application to low-consumption electricity transmission.

VI. GAUGE INVARIANCE

We find that $\boldsymbol{j}_5$ and ρ_5 are proportional to $\partial_t \boldsymbol{S}$ from Eqs. (11) and (12) because of the gauge invariance in the doped DS. Owing to spin-momentum locking, $\boldsymbol{S}$ plays a role like the electromagnetic vector potential as $\mathcal{H}_{\mathrm{W},\gamma} + \mathcal{H}_{\mathrm{ex},\gamma} \propto \boldsymbol{\sigma} \cdot (\boldsymbol{k} - \frac{e}{\hbar}\boldsymbol{\mathcal{A}}_\gamma)$, where the vector potential $\boldsymbol{\mathcal{A}}_\gamma = J_{\mathrm{ex}}\boldsymbol{S}/(e v_{\mathrm{F},\gamma})$ is conjugate to $\boldsymbol{j}_\gamma$. Therefore, the observable quantity should be proportional to the gauge-invariant form as $-\partial_t \boldsymbol{\mathcal{A}}_\gamma \equiv \boldsymbol{\mathcal{E}}_\gamma$ or $\nabla \times \boldsymbol{\mathcal{A}}_\gamma \equiv \boldsymbol{\mathcal{B}}_\gamma$ [33]. The axial current and charge are driven by an effective electric field $\boldsymbol{\mathcal{E}}_\gamma$ and $\nabla \cdot \langle \boldsymbol{\mathcal{E}}_\gamma \rangle_{\mathrm{D}}$, respectively, as shown from Eqs. (11) and (12).

VII. SUMMARY

In conclusion, we have studied the nonequilibrium axial current density $\boldsymbol{j}_5$ and axial charge density ρ_5 based on a Green's function technique in the MI/doped DS junction. We have found that $\boldsymbol{j}_5$ is driven by the DCSE due to $\partial_t \boldsymbol{S}$, as expected from the gauge invariance of $\boldsymbol{S}$. $\boldsymbol{j}_5$ can be decomposed into the local and diffusive ones. Based on our results, we have discussed a procedure for the detection of the local and diffusive axial current by using the magnetic resonance and the inverse spin Hall effect, respectively [34]. The DCSE induces $\boldsymbol{j}_5$ with no accompanying charge transport, and $\boldsymbol{j}_5$ can be converted into charge current in the MI/doped DS/NM junction. These properties of $\boldsymbol{j}_5$ can be useful for the application of DS to low-consumption electronics. Thus, the present paper has explored a new area of the axial-current-based electronics, *axitronics*.

ACKNOWLEDGMENTS

The authors are grateful to K. Nomura, K. Yada, A. Yamakage, S. Kobayashi, and L. Bo for fruitful comments. This work was supported by Grants-in-Aid for Young Scientists (B) (No. 22740222 and No. 23740236) by Grants-in-Aid for Scientific Research on Innovative Areas "Topological Quantum Phenomena" (No. 22103005 and No. 25103709) from the Ministry of Education, Culture, Sports, Science, and Technology, Japan (MEXT), and by the Core Research for Evolutional Science and Technology (CREST) of the Japan Science and Technology Corporation (JST). K.T. acknowledges support from a Grant-in-Aid for Japan Society for the Promotion of Science (JSPS) Fellows.

[1] Y. Tserkovnyak, A. Brataas, and G. E. W. Bauer, Phys. Rev. Lett. **88**, 117601 (2002).
[2] Y. Tserkovnyak, A. Brataas, and G. E. W. Bauer, Phys. Rev. B **67**, 140404(R) (2003).
[3] A. Takeuchi, K. Hosono, and G. Tatara, Phys. Rev. B **81**, 144405 (2010).
[4] S. Maekawa, H. Adachi, K. Uchida, J. Ieda, and E. Saitoh, J. Phys. Soc. Jpn. **82**, 102002 (2013).
[5] S. Takahashi and S. Maekawa, J. Phys. Soc. Jpn. **77**, 031009 (2008).
[6] Y. Kajiwara *et al.*, Nature (London) **464**, 262 (2010).
[7] T. Kimura, Y. Otani, T. Sato, S. Takahashi, and S. Maekawa, Phys. Rev. Lett. **98**, 156601 (2007).
[8] E. Saitoh, M. Ueda, H. Miyajima, and G. Tatara, Appl. Phys. Lett. **88**, 182509 (2006).
[9] K. Ando, S. Takahashi, K. Harii, K. Sasage, J. Ieda, S. Maekawa, and E. Saitoh, Phys. Rev. Lett. **101**, 036601 (2008).
[10] A. Vilenkin, Phys. Rev. D **22**, 3080 (1980).
[11] M. A. Metlitski and A. R. Zhitnitsky, Phys. Rev. D **72**, 045011 (2005).
[12] G. M. Newman and D. T. Son, Phys. Rev. D **73**, 045006 (2006).
[13] D. Kharzeev and A. Zhitnitsky, Nucl. Phys. A **797**, 67 (2007).
[14] D. E. Kharzeev, L. D. McLerran, and H. J. Warringa, Nucl. Phys. A **803**, 227 (2008).
[15] E. V. Gorbar, V. A. Miransky, I. A. Shovkovy, and Xinyang Wang, Phys. Rev. D **88**, 025025 (2013).
[16] D. Kharzeev, K. Landsteiner, A. Schmitt, and H.-U. Yee, *Strongly Interacting Matter in Magnetic Fields* (Springer, New York, 2013), Chap. 9.
[17] Y. Chen, S. Wu, and A. A. Burkov, Phys. Rev. B **88**, 125105 (2013).
[18] A. A. Zyuzin, S. Wu, and A. A. Burkov, Phys. Rev. B **85**, 165110 (2012).
[19] The chiral separation effect exits only at nonzero chemical potential for the fermions [11].
[20] D. E. Kharzeev, Prog. Part. Nucl. Phys. **75**, 133 (2014).
[21] S. Murakami, New J. Phys. **9**, 356 (2007).
[22] A. A. Burkov and L. Balents, Phys. Rev. Lett. **107**, 127205 (2011).
[23] J. Tominaga, A. V. Kolobov, P. Fons, T. Nakano, and S. Murakami, Adv. Mater. Interfaces **1**, 1300027 (2014).
[24] H. Haug and A. P. Jauho, in *Quantum Kinetics in Transport and Optics of Semiconductors*, 2nd ed. (Springer, New York, 2007), pp. 45–46.
[25] The diffusion propagation function $\mathcal{D}(\boldsymbol{x},t) = \frac{\theta(t)\sqrt{\pi}}{\pi^2 \ell_{\mathrm{D}}^3} \exp[-x^2/\ell_{\mathrm{D}}^2]$ exponentially decays with a diffusive length $\ell_{\mathrm{D}}(t) = \sqrt{6Dt}$.
[26] Here $\boldsymbol{j}_5$ is conserved unless there are simultaneously electric field and magnetic field parallel to each other in the junction.
[27] We find that in the doped DS, ρ_5 is proportional to the spin current $j_{\mathrm{s},i}^{\alpha}$ as $j_{\mathrm{s},i}^{\alpha} \propto v_{\mathrm{F}} \rho_5 \delta_{i\alpha}$, where the spin current is defined by $\partial_t s^\alpha + \nabla_i j_{\mathrm{s},i}^{\alpha} = \mathcal{T}^\alpha$ and $\mathcal{T}^\alpha$ is a spin relaxation.

[28] S. Chikazumi, *Physics of Ferromagnetism* (Oxford University Press, New York, 1997), Chaps. 20 and 21.

[29] S. Mizukami, Y. Ando, and T. Miyazaki, Phys. Rev. B **66**, 104413 (2002).

[30] Then, the spin current $j^{\alpha}_{s,i} \propto \rho_5 \delta_{i\alpha}$ is also zero and does not contribute to the magnetization dynamics.

[31] The diffusion equation is given by acting the differential equation of $\mathcal{D}$ onto $\boldsymbol{j}^{\mathrm{D}}_5$ from the left side, where the differential equation is defined by $(\partial_t - \frac{3}{2}D\nabla^2)\mathcal{D}(\boldsymbol{x}-\boldsymbol{x}', t-t') = \delta(t-t')\delta^3(\boldsymbol{x}-\boldsymbol{x}')$.

[32] The property of $\boldsymbol{j}^{\mathrm{D}}_5$ is similar to that of the spin current in metals. However, $\boldsymbol{j}^{\mathrm{D}}_5 = -\frac{3}{2}D\boldsymbol{\nabla}\rho_5$ is not equal to spin current in the doped DS as shown in Ref. [27]. Besides, $\boldsymbol{j}^{\mathrm{D}}_5 \propto \boldsymbol{s}^{\mathrm{D}}$ satisfies the spin conservative form as $\partial_t s^{\mathrm{D},i} + \partial_a j^{\mathrm{D,i}}_a = 0$, where $j^{\mathrm{D,i}}_a$ is a flow of spin and is not equal to the spin current in the doped DS.

[33] Similarly to the quantum anomaly due to the electromagnetic field, one can expect that the effective electromagnetic field triggers the quantum anomaly $\partial_t \rho_5 + \boldsymbol{\nabla}\cdot\boldsymbol{j}_5 = -\frac{eJ^2_{\mathrm{ex}}}{2\pi^2\hbar^2 v^2_{\mathrm{F}}}\partial_t \boldsymbol{S}\cdot(\boldsymbol{\nabla}\times\boldsymbol{S})$. When $\partial_t\boldsymbol{S}\cdot(\boldsymbol{\nabla}\times\boldsymbol{S})$ is zero as realized in a transverse conical spin wave, the axial current is a conservative flow. If the magnitude of J_{ex} is negligibly small, i.e., $\frac{J^2_{\mathrm{ex}}}{\hbar^2 v^2_{\mathrm{F}}} \ll 1$, the axial current can be regarded as a conservative flow. In addition, one can expect that the effective electromagnetic field contributes to the quantum anomaly for the charge conservation as $\partial_\mu j^\mu \propto \partial_t\boldsymbol{S}\cdot\boldsymbol{B}$ in the junction. Here the magnetic field $\boldsymbol{B}$ is assumed to be the magnetization $\boldsymbol{M} \propto -\boldsymbol{S}$ in the doped DS in the absence of the applied magnetic field. When $|\boldsymbol{S}|^2$ is independent of time, we expect that the relation $\partial_t\boldsymbol{S}\cdot\boldsymbol{B} \propto \partial_t|\boldsymbol{S}|^2 = 0$ is satisfied and the anomaly is not triggered in the junction we consider.

[34] We find that axial current is a special flow in DS. Although the axial current can transport spin degrees of freedom without spin relaxation, it is different from spin current. Spin current is not conservative flow, while the axial current is conservative flow and can be observable. Axial current is also different from valley current in graphene. Valley current could not be controlled by magnetic field or magnetization. On the other hand, it is possible to manipulate the axial current by using the spin degree of freedom.